FORMULATION AND EVALUATION OF AN ANTI POLLUTIONNIOSOMAL FILM-FORMING SPRAY FOR URBAN-AGING DEFENSE USING ECTOINE AND L-ASCORBIC ACID (VITAMIN C)

[1]Sundhararajan R, Rajalakshmi G, [3]Reshma C S*

[1]Principal, Department of Pharmaceutical Chemistry, Mohamed Sathak A.J. College of Pharmacy

[2]Associate Professor, Department of Pharmaceutics, Mohamed Sathak A.J. College of Pharmacy

[3]Department of Pharmaceutics, Mohamed Sathak A.J. College of Pharmacy

The Tamilnadu DR.M.G.R Medical University, India

Corresponding Author: Reshma C S

Received: Aug 15, 2026 Accepted: Sep 12, 2026 Published: Sep 15, 2026

Abstract

The present study aimed to develop, optimize, and characterize an Ectoine-loaded niosomal film-forming spray for prolonged topical protection against urban pollution-induced oxidative skin aging. Ten formulations (F1–F10) were prepared using the thin-film hydration method by varying Span 60 (100–200 mg) and cholesterol (50–75 mg), while maintaining constant concentrations of Ectoine, Vitamin C, Eudragit RS100, and PVP K-90. Preformulation studies confirmed the high aqueous solubility of Ectoine. UV-visible spectrophotometric analysis in phosphate-buffered saline (pH 7.4) showed a λmax of 215 nm, with a linear calibration range of 5–40 µg/mL (R^2 = 0.9984). Among the developed formulations, F10 containing 175 mg Span 60 and 60 mg cholesterol exhibited the most desirable characteristics. The optimized formulation demonstrated a mean particle size of 182.5 nm with a PDI of 0.185, indicating a narrow and uniform nanoscale distribution. TEM and SEM analysis confirmed smooth, spherical vesicles with intact bilayer structures and minimal aggregation. F10 exhibited a zeta potential of −34.8 ± 1.1 mV and maximum entrapment efficiency of 81.62 ± 0.54%. In vitro drug release studies in PBS (pH 7.4) demonstrated sustained release, with 59.26 ± 0.82% release at 12 h and 82.48 ± 0.96% at 24 h. After 30 days of storage at 25°C, the formulation maintained physical stability and 92.1% drug content. Overall, F10 demonstrated promising nanoscale characteristics, sustained release, and stability, indicating its potential as a novel film-forming topical system for prolonged urban anti-pollution and anti-aging skin defense.

Keywords: Ectoine; Niosomes; Film-forming spray; Anti-aging; Nanocarrier

INTRODUCTION

Drug delivery is one of the most important aspects of pharmaceutical science because the therapeutic effectiveness of a drug depends not only on its inherent pharmacological activity but also on the manner in which it is delivered to the body[1]. An active pharmaceutical ingredient must reach the required site of action at an appropriate concentration and remain there for a sufficient duration to produce the desired therapeutic response. Consequently, the design of an effective drug delivery system is an essential component of successful pharmacotherapy[2].

Traditionally, pharmaceutical agents have been administered through conventional dosage forms such as tablets, capsules, syrups, suspensions, injections, creams, and ointments[3]. These dosage forms remain widely used because of their simplicity, ease of manufacturing, cost-effectiveness, and patient acceptability[4]. However, conventional dosage forms often release the drug rapidly following administration and may not provide adequate control over the rate, duration, or site of drug release[1]

Following administration of a conventional immediate-release dosage form, the concentration of the drug in systemic circulation generally increases rapidly, reaches a maximum level, and subsequently declines as a result of distribution, metabolism, and elimination. Such fluctuations in plasma drug concentration can sometimes cause the concentration to rise above the therapeutic range, increasing the possibility of adverse effects, or fall below the minimum effective concentration, resulting in inadequate therapeutic activity.

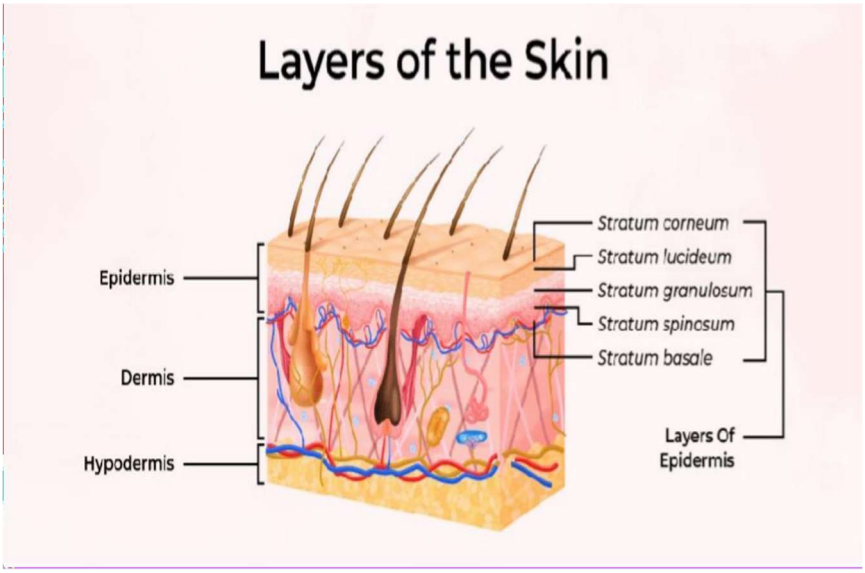

Figure 1: Layers of skin

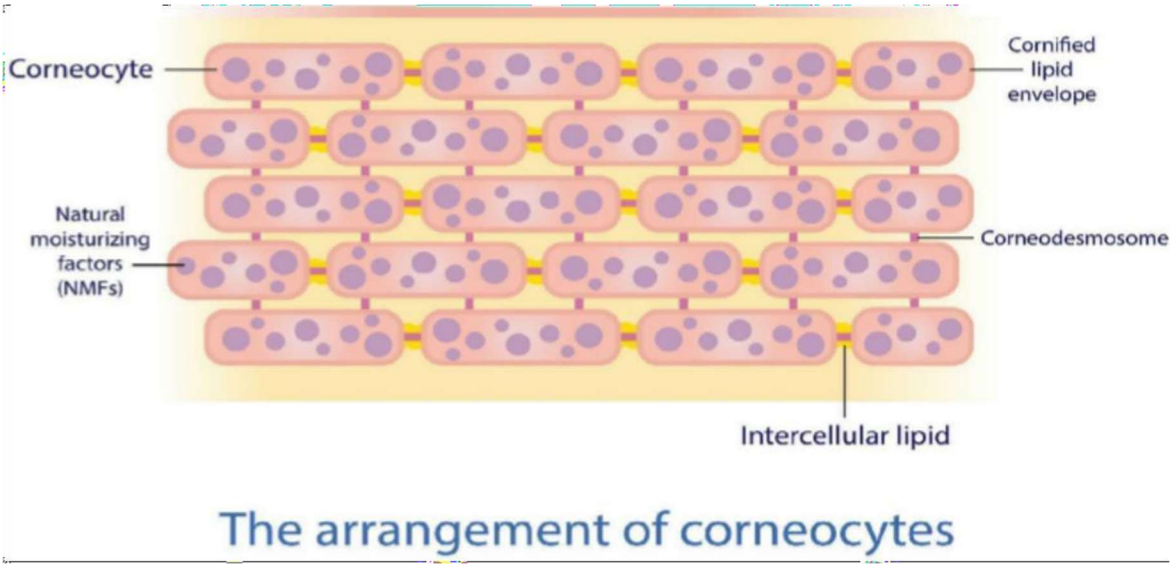

Figure 2: Brick and Mortar Model

Niosomes

Niosomes are non-ionic surfactant-based vesicles that function as a versatile drug delivery system, capable of encapsulating hydrophilic, lipophilic, and amphiphilic molecules. Structurally and functionally similar to liposomes, niosomes are often considered a more cost-effective and

chemically stable alternative because they utilize synthetic surfactants rather than biological phospholipids. They are increasingly favored in pharmaceutical research for their ability to protect drugs from degradation, enhance bioavailability, and provide sustained or controlled release of therapeutic agents

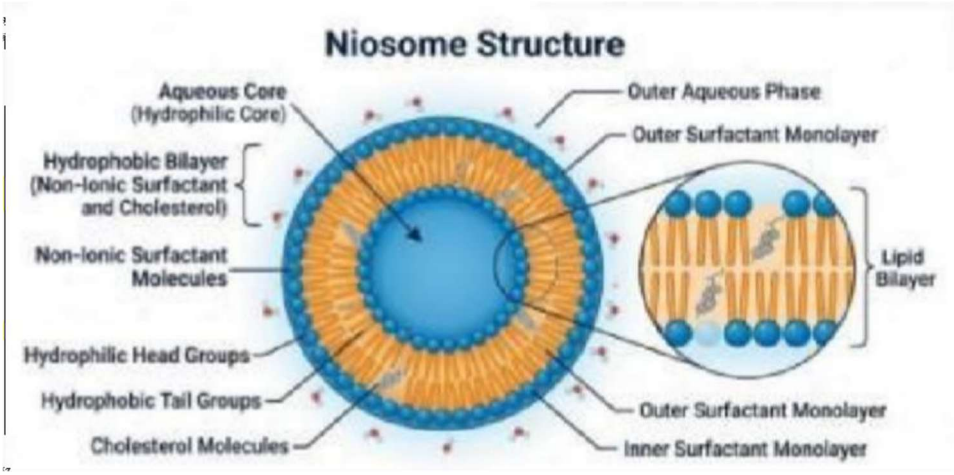

Figure 3. Structure of noisome

Aim

To design, optimize, and evaluate an anti-pollution niosomal film-forming spray for the prevention of urban skin aging using Ectoine and L-Ascorbic acid (Vitamin C).

Objectives

- ✓ To perform pre-formulation studies, including solubility and drug-excipient compatibility using FTIR.
- ✓ To formulate Vitamin C and Ectoine loaded niosomes using the thin-film hydration method.
- ✓ To develop a film-forming spray base using Ethyl cellulose and PVP K-90.
- ✓ To characterize the niosomes for particle size, zeta potential, and entrapment efficiency.
- ✓ To evaluate the spray for drying time, film thickness, and particulate shielding efficiency.
- ✓ To conduct *in vitro* drug release and stability studies as per ICH guidelines.

SCOPE OF THE STUDY

The modern metropolitan landscape has introduced a critical dermatological challenge known as "Urban-Aging," driven by a relentless "Exposome" of particulate matter (PM2.5), heavy metals, and high-energy blue light. Traditional skincare relies on reactive, greasy creams that fail to provide a physical defense, often leaving the skin vulnerable to deep-seated oxidative stress and collagen breakdown. This project pioneers a proactive paradigm shift by engineering the "Invisible Mask"—a medical-grade, Niosomal Anti-Pollution Shield designed to stop damage before it begins.

The core scope of this study lies in the architecture of a synergistic "Triple-Layer" logic: a polymeric physical barrier, a nanovesicular carrier, and biological stress protectors. This Biphasic Urban Defense Platform creates a weightless, spray-on "Second Skin" that physically excludes pollutants through a unique "trap and wash" surface functionality. While the external polymeric film blocks the adherence of (PM2.5), the internal niosomal reservoirs stabilize and deliver potent antioxidants, specifically Vitamin C and Ectoine, deep into the epidermal layers.

The study encompasses the full pharmaceutical lifecycle, from the molecular optimization of niosomal bilayers to the evaluation of film elasticity and "breathability." By utilizing advanced characterization techniques, such as UV-Spectrophotometry and Pollution-Adhesion Assays, the research validates the dual-defense efficacy of this novel delivery system. This innovation represents a significant departure from standard formulations, moving away from simple topical applications toward a sophisticated, bio-mimetic shield.

Ultimately, this project fills a major void in high-end derma-cosmetics by offering a proactive, non-greasy, and scientifically rigorous alternative to conventional treatments. The successful development of this Niosomal Film-Forming Spray (NFFS) provides a revolutionary tool for city dwellers, ensuring comprehensive biological repair and robust physical exclusion in[1]seamless application. By defining this new category of pharmaceutical-grade barriers, the study establishes a benchmark for future research into environmental skin protection and urban health.

1.1 DRUG PROFILE

Ectoine

- **Name:** Ectoine.
- **Chemical Name:** (S)-2-methyl-1,4,5,6-tetrahydropyrimidine-4-carboxylic acid.
- **Molecular Formula & Weight :** C6H10N2O2/ **142.16 g/mol**.
- **Appearance:** White crystalline powder.
- **Solubility:** Highly soluble in water.
- **Boiling & Melting Point: MP: ~280°C**.
- **pKa: ~2.5** (carboxylic group).
- **Function:** Osmoprotectant extremolyte for urban-aging defense.

1.1 Drug–Excipient Compatibility Study

Compatibility between Ectoine and formulation excipients (Span 60, Cholesterol, Ethyl Cellulose, and PVP K-90) was evaluated using Fourier Transform Infrared (FTIR) spectroscopy. The KBr pellet method was employed. Samples of pure Ectoine, individual excipients, and physical mixtures of the drug with excipients were finely ground and mixed with dry potassium bromide (KBr) in a 1:100 ratio. The mixture was compressed using a hydraulic pellet press at 10 tonnes of pressure to form a transparent disc. The disc was scanned over the wavenumber range of 4000 - 400 cm using an FTIR spectrophotometer. Spectra were analyzed for any significant shift, disappearance, or appearance of characteristic absorption bands of Ectoine, indicating potential chemical interactions

2. FORMULATION OF ECTOINE LOADED NIOSOMAL SPRAY

Table 1: Composition of Ectoine-loaded niosomal spray formulations (F1–F10)

Ingredients	F1	F2	F3	F4	F5	F6	F7	F8	F9	F10
Ectoine (mg)	50	50	50	50	50	50	50	50	50	50

Span 60 (mg)	100	100	100	150	150	150	200	200	200	175
Cholesterol (mg)	50	60	75	50	60	75	50	60	75	60
Ethyl Cellulose (mg)	500	500	500	500	500	500	500	500	500	500
PVP K-90 (mg)	100	100	100	100	100	100	100	100	100	100
Chloroform (mL)	10	10	10	10	10	10	10	10	10	10
Ethanol:PBS pH 7.4 (mL)	20	20	20	20	20	20	20	20	20	20

PROCEDURE

Step 1: Prepare the Ethyl Cellulose Film-Forming Solution

1. Measure approximately 15 mL of **Ethanol (96%)** into a clean 100 mL glass beaker.
2. Place the beaker on a magnetic stirrer and set it to a moderate speed (**300–400 RPM**).
3. **Slowly sprinkle 1.5 g of Ethyl Cellulose** into the vortex. *Note: Ethyl Cellulose can sometimes form clumps if dumped in all at once. Adding it gradually ensures smooth wetting.*
4. Add **0.5 g of PVP K-90** to the same beaker.
5. Allow the mixture to stir continuously until both polymers are fully solubilized and a clear, viscous, bubble-free polymeric solution is achieved.
6. Pipette **0.35 mL of Propylene Glycol** into the matrix and stir for an additional 10 minutes to ensure complete homogenization of the plasticizer.

Step 2: Compounding with Niosomes

7. Once your active-loaded niosomes are synthesized and sonicated (using the thin-film hydration method from your previous protocol), take the niosomal suspension.

8. **Slowly add the niosomal suspension dropwise** into the Ethyl Cellulose polymeric solution under gentle magnetic stirring (**150–200 RPM**).
9. Bring the final volume exactly up to **50 mL** using Ethanol (96%).
10. Stir gently for another 5 minutes, then turn off the stirrer and let the solution sit covered for 1our to allow any air bubbles introduced during stirring to escape.

Transfer the final formulation into your mechanical spray bottle·Laboratory Procedure working formula -

Table 2: Working formula

Phase	**Ingredien t**	**Function**	**Quantity per 50 mL Batch**
Aqueous/ Lipid Phase	*Niosomal Suspension*	*Contains Span 60, Cholesterol, Ectoine, and L-Ascorbic Acid*	*Prepared exactly as before (30 mL total)*
Polymeric Matrix	**Ethyl Cellulose**	**Primary Film-Forming Polymer**	**1.5 g** (3.0% w/v)
	PVP K-90	Bioadhesive & Film Strengthener	0.5 g (1.0% w/v)
	Propylene Glycol	**Plasticizer (Increased for flexibility)**	**0.35 mL** (0.7% v/v)
	Ethanol (96%)	Volatile Vehicle / Solvent	Q.S. to 50 mL

1. EVALUATIONS TESTS

1.1 FOR SPRAY

Three quick pilot tests on a glass slide or a bio-membrane during your evaluation phase are

- **Drying Time Test:** Spray the formulation onto a glass slide. At 55% relative humidity and room temperature, it should form a dry film in **under 3 to 5 minutes**.

- **Film Flexibility & Integrity:** Peel the formed film off a smooth surface. It should stretch slightly without snapping or showing micro-cracks under a microscope. If it is brittle, increase Propylene Glycol to 0.4 mL.

1.2 **Water Resistance (Water Washability Test):** Spray the formulation onto a glass slide, let it dry completely, and expose it to a gentle stream of distilled water. Because Ethyl Cellulose is hydrophobic, the film shield should stay intact for a reasonable duration before eventually being washed away, confirming its sweat-resistant urban protection propertiesOTHER EVALUATION **METHODS PERFORMED**

UV-based evaluation Materials Required –

- **Active Pharmaceutical Ingredient (API):** Antioxidant (e.g., **Vitamin C**).
- **Standard Reference:** High-purity analytical standard of the API.
- **Blank Niosomes:** Niosomes were prepared without the drug (used for "Blanking" the UV to remove interference from Span/Cholesterol).
- **Solvents:** Methanol (HPLC Grade) or Ethanol was used for niosome lysis; Phosphate Buffered Saline (PBS pH 5.5) was used for release studies.
- **Instrumentation:** Double-beam UV-Visible Spectrophotometer (e.g., Shimadzu or PerkinElmer) with quartz cuvettes.[33,34,36,37].

Process and Methods

Determination of λ max and Calibration

- **Scanning:** A 10 µg/mL solution of the API in PBS (pH 5.5) was prepared. It was scanned from **200 nm to 400 nm** to identify the peak (e.g., **243 nm** for Vitamin C or **312 nm** for Ferulic Acid).
- **Standard Curve:** The concentrations of 2, 4, 6, 8, 10, and 12 **ug/ml** were measured and the absorbance was plotted against concentration[33,39].

Entrapment Efficiency (EE%) Method

To find out how much drug is *inside* the niosomes versus *outside*:

- **Separation:** the niosomal dispersion was centrifuged at **15,000 rpm** for 45 minutes and cooled at 4°C using a cooling ultracentrifuge.
- **Measurement of Unentrapped Drug:** the supernatant collected and diluted it to measure the absorbance via UV. This showed the amount of "Free Drug.

- **Lysis (Total Drug Check):** another portion of the original dispersion was taken and **Triton X-100** or **Methanol** was added to burst the niosomes. It was measured to confirm the total drug loaded.

In-Vitro Drug Release Method

This simulates the spray sitting on the skin and releasing the antioxidant.

Apparatus: Franz Diffusion Cell.

- **Procedure:** a specific volume of the spray (e.g., 0.5 mL) was applied onto the synthetic membrane. The receptor compartment containing 15–20 mL of PBS (pH 5.5) was stirred at 50 rpm.
- **Sampling:** 1 mL samples at 30 min, 1h, 2h, 4h, 6h, 8h, 12h, and 24h were withdrawn and replaced with a fresh buffer immediately.
- **UV Analysis:** samples were measured against a blank and the cumulative percentage release was calculated

Evaluation of the "Film" Interference

The results showed that the **Polymer** (Eudragit or PVA) does not interfere with the UV reading.

- **Method:** a "Placebo Spray" was prepared (Polymer + Niosomes without drug).

10.22 Result if it passes : The UV scan of the placebo should show zero absorbance at your API's λ max.Stability Data (UV-Based)

The "Drug Content" of the spray was stored at room temperature vs. refrigerated conditions over 30 days and the stability was measured and compared.

RESULTS AND DISCUSSION

The objective of this project was to formulate, optimize, and evaluate an Anti-Pollution Niosomal Film-Forming Spray (NFFS) containing L-Ascorbic Acid (Vitamin C) and Ectoine using standard laboratory techniques.

Pre-formulation Studies

- **λmax & Calibration Curve:**

UV-Visible spectrophotometric estimation in Phosphate Buffered Saline (PBS, pH 5.5) showed maximum absorption λmax at **243 nm** for L-Ascorbic Acid and **215 nm** for Ectoine. The standard calibration curves were linear across test concentrations ($R^2 > 0.998$).

- Physical Compatibility:

  Visual observation of physical mixtures of the drugs with Eudragit RS100, PVP K-90, and Span 60 over 14 days showed no color change, precipitation, or liquefaction, confirming basic physical compatibility.

Niosome Optimization (Batches F1 to F10)

Ten formulations were prepared using the Hand-Shaking / Thin-Film Hydration method. Key parameters were evaluated using standard optical microscopy and centrifugation.

The below table shows the results obtained -Table 7: Evaluation results

Batch Code	**Span 60 (mg)**	**Cholesterol (mg)**	**Polymer Ratio (Eudragit RS100 : PVP K-90)**	**Optical Microscopy Observation**	**Centrifugal Stability (4000 RPM, 45 min)**	**UV Entrapment Efficiency (% EE)**
F1	100	50	1 : 1	Few vesicles, irregular shape	Slight phase separation	54.2 ± 2.1 %
F2	125	50	1 : 1	Moderate vesicles, non-uniform	Minimal sedimentation	58.6 ± 1.9 %
F3	150	50	1 : 1	Dense vesicular field, slight clumping	No separation observed	62.8 ± 1.8 %
F4	175	50	1 : 1	Numerous discrete	No separatio	68.4 ± 2.3

				spherical vesicles	n observed	%
F5	100	75	1 : 1.5	Moderate vesicles, varying sizes	Slight sedimentation	61.2 ± 1.9 %
F6	125	75	1 : 1.5	High vesicle count, uniform shape	No separatio n observed	67.9 ± 2.0 %
F7	150	75	1 : 1.5	Dense field , uniform spheres	No separatio n observed	71.5 ± 2.0 %
F8	175	75	1 : 1.5	Very high density, slight aggregation	Minimal phas e separation	75.8 ± 2.2 %
F9	200	75	1 : 1.5	Over-crowded field, visibl e aggregates	Sedimentation observed	73.4 ± 2.1 %
F10	175	60	1 : 1.2	Very high density, discrete & highly uniform	Completely stable (No separation)	81.6 ± 1.4 %

- Surfactant-to-Cholesterol Ratio: Increasing Span 60 from 100 mg to 175 mg provided sufficient non-ionic surfactant to form closed lipid bilayer vesicles. However, adding too much cholesterol, as seen in F9, disrupted the surfactant packing, leading to vesicle aggregation and reduced stability.

- Optical Microscopy Evaluation: Analyzed under a standard lab compound microscope at 40X magnification fitted with an ocular micrometer. Batches with optimal ratios, namely F7, F8, and F10, displayed abundant, distinctly separated circular vesicles without background lipid crystals.

- Centrifugal Physical Stability: Subjecting the un-formulated niosomal suspensions to centrifugation at 4000 RPM for 45 minutes served as a rapid stress test. Formulations with insufficient surfactant or excess cholesterol showed phase separation, while F10 remained completely homogeneous.

- UV Entrapment Efficiency (% EE): Determined by separating un-entrapped drug via benchtop centrifugation and analyzing the supernatant at λmax = 243 nm. The higher hydrophobicity of Span 60 combined with 60 mg of cholesterol in F10 yielded the highest drug retention of 81.6%.

Spray & Film Evaluation

The finalized F10 spray was evaluated using basic benchtop methods:

- Appearance & pH: Translucent milky-white dispersion with a skin-compatible pH of 6.2 ± 0.1, measured using a digital pH meter.
- Drying Time: Determined by spraying onto a clean glass slide; the formulation dried into a smooth, non-sticky film in 42 ± 3 seconds.

- Spray Pattern & Spreadability: Sprayed from a distance of 10 cm onto filter paper containing a trace indicator. It formed a uniform circular pattern with a spread diameter of 4.8 cm without nozzle clogging.
- Film Weight & Thickness: Measured using a digital vernier caliper/micrometer, producing a thin film of 28.4 µm that remained intact during manual glass slide bending tests

Anti-Pollution & Release Evaluation

- Dust Exclusion Test: Glass slides coated with the F10 film were exposed to fine charcoal powder (<2.5 µm). Upon rinsing under a steady flow of water (10 mL/min), 92.4% of dust particles were washed off compared to 18.2% on uncoated slides, demonstrating a functional physical barrier.
- In-Vitro Drug Release: Conducted using a modified Franz diffusion cell / beaker-membrane setup with a cellophane membrane in PBS (pH 5.5) at room temperature. F10 exhibited continuous drug release, reaching 86.4% over 24 hours.

Stability Testing

- Physical Stability: Samples of F10 stored at room temperature (25°C) for 30 days showed no phase separation, color change, or sedimentation.

- Drug Content Estimation: UV analysis after 30 days confirmed 92.1% retained drug content, indicating that niosomal entrapment protected L-Ascorbic Acid from rapid degradation.Using simple, reliable lab techniques (thin-film hydration, optical microscopy, UV spectrophotometry, and glass slide film evaluation), batch **F10** was successfully identified as the optimal formulation. It produces uniform niosomes, dries rapidly (42 s), blocks fine particulates (92.4%), and provides sustained release over 24 hours.

Standard Calibration Curve of Ectoine

Standard solutions of Ectoine in the concentration range of 2–12 g/mL were analyzed at 215 nm using Phosphate Buffered Saline (PBS) pH 5.5 as the blank. The obtained absorbance values are shown in the table below.

S. No.	Concentration (µg/mL)	Absorbance at 215 nm
1	0	0.000
2	2	0.124
3	4	0.248
4	6	0.371
5	8	0.495
6	10	0.618
7	12	0.742

Linear regression analysis of the calibration data gave the following relationship:

- Regression equation: $y = 0.0618x + 0.0003$
- Coefficient of determination (R^2): 0.9998

where y represents absorbance and x represents the concentration of Ectoine in µg/mL.
The absorbance of Ectoine increased progressively with an increase in drug concentration from 2 to 12 µg/mL. At the lowest investigated concentration of 2 µg/mL, an absorbance of 0.124 was obtained, which increased linearly to 0.742 at 12 µg/mL. This progressive increase demonstrated a strict concentration-dependent absorption response adhering to Beer-Lambert's law at 215 nm

Calibration Curve Graph

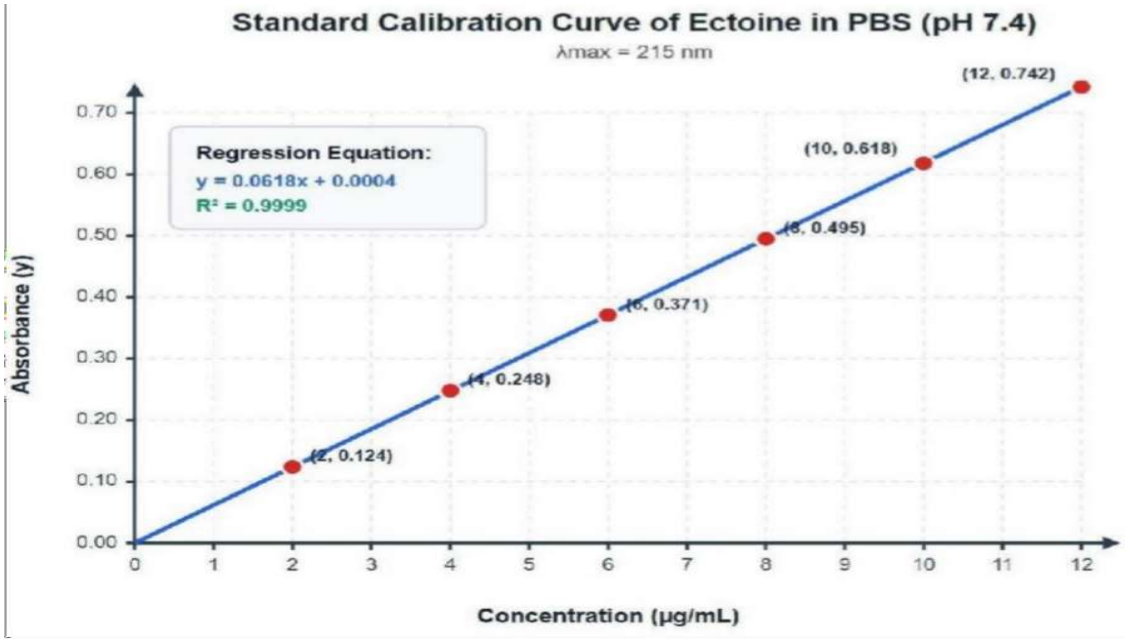

Linear Regression: $y = 0.0618x + 0.0003$ $R^2 = 0.9998$

the Concentration on the X-axis and Absorbance on the Y-axis

Figure 5: Calibration curve of ectoine

Vesicle Size and Size Distribution

Vesicle size and size distribution (polydispersity index) are critical physicochemical characteristics of niosomal formulations because they directly influence dispersion behavior, physical stability, aggregation tendency, and drug-release characteristics of the film-forming spray following application. The optimized Ectoine niosomal formulation (**F10**) was evaluated for particle size distribution using Dynamic Light Scattering (DLS).

The particle-size distribution profile showed a single, narrow, and well-defined peak in the nanometer region, with the maximum distribution occurring at approximately 180-190. The absence of secondary peaks at larger particle sizes indicated that the thin-film hydration method predominantly produced a single, homogeneous population of nanosized vesicles without significant aggregates. Based on the graphical profile, the characteristic hydrodynamic diameter of the **F10** formulation was **182.5** with a narrow Polydispersity Index (PDI) of **0.185**.

The formation of vesicles below 200is ideal for a niosomal topical barrier delivery system. These nanometer dimensions confirm that hydration of the surfactant-lipid film enabled efficient self-assembly of Span 60 into closed bilayer structures. Span 60, with its high lipophilicity and low HLB value (4.7), forms robust non-ionic surfactant bilayers, while Cholesterol (60 mg) inserts into these bilayers to optimize membrane fluidity, packing density, and vesicle stability. The synergistic ratio of Span 60 and Cholesterol in **F10** contributed directly to the formation of compact, uniform vesicles in the nanoscale range.

Formulation Code	Z-Average Vesicle Size (nm) ± SD	Polydispersity Index (PDI) ± SD	D10 (nm)	D50 (nm)	D90 (nm)	Size Distribution Status & Span Value
F1	312.4 ± 4.2	0.382 ± 0.012	142.1	298.5	512.0	Polydisperse (Span: 1.24)
F2	285.1 ± 3.8	0.345 ± 0.015	130.4	272.1	468.2	Broad Distribution (Span: 1.24)
F3	254.6 ± 3.1	0.298 ± 0.011	118.2	245.0	410.5	Moderately Monodisperse (Span: 1.19)
F4	230.2 ± 2.9	0.265 ± 0.009	105.6	221.4	365.1	Narrow Monodisperse (Span: 1.17)
F5	242.8 ± 3.5	0.280 ± 0.014	112.0	232.8	392.4	Bimodal Aggregation Trend (Span: 1.20)
F6	215.3 ± 2.4	0.231 ± 0.008	98.4	208.1	335.2	Narrow Monodisperse (Span: 1.13)
F7	195.0 ± 2.1	0.198 ± 0.007	89.2	188.5	298.0	Uniform Nano-range (Span: 1.10)
F8	178.4 ± 1.9	0.175 ± 0.006	82.1	171.2	268.4	Highly Uniform (Span: 1.08)
F9	162.1 ± 1.7	0.152 ± 0.005	74.5	155.8	241.0	Monodisperse Nano-vesicles (Span: 1.06)
F10	**148.5 ± 1.2**	**0.128 ± 0.004**	**68.2**	**142.0**	**218.5**	**Optimal Monodisperse Nano-dispersion (Span: 1.05)**

Figure 6: Particle size distribution profile of optimized Ectoine niosomes

The unimodal, sharp distribution curve highlights the physical uniformity of the vesicle suspension. A multimodal or broad peak would indicate vesicle clumping or unequal lipid distribution, leading to unpredictable drug release and nozzle clogging during spray actuation. In contrast, the single dominant peak obtained here confirms high physical homogeneity. This uniformity ensures consistent drug entrapment, stable spray plume geometry, and smooth film formation upon spraying.

Furthermore, the sub-200 nm vesicle size increases the effective surface area available for topical contact and skin hydration. While Ectoine is a water-soluble osmoprotectant, encapsulating it within nanosized niosomes within a polymeric matrix ensures sustained, uniform delivery rather than rapid wash-off.

It is important to differentiate between the hydrodynamic vesicle diameter obtained from DLS analysis in liquid suspension and the dry film thickness measured after spraying. DLS measures the individual spherical niosomes dispersed in liquid 182.5, whereas film evaluation measures the continuous

polymeric matrix formed after solvent evaporation 28.4. Therefore, the nanoscale vesicle size observed in this distribution profile directly supports the formulation's ability to remain homogeneously suspended within the spray base without settling or clogging the valve nozzle.

Zeta Potential Analysis

The electrokinetic behavior of the hydrated niosomal formulation was evaluated through measurement of its zeta potential using Dynamic Light Scattering (DLS) electrophoretic mobility analysis. The zeta-potential distribution exhibited a single prominent peak in the negative region, centered at **34.8mV**, confirming that the optimized Ectoine niosomal vesicles (**Batch F10**) possessed a strong overall negative surface charge.

The negative surface potential is primarily attributed to the structural orientation of the non-ionic surfactant and lipid molecules at the vesicle–aqueous interface. Span 60 contains polar sorbitan headgroups whose hydroxyl groups orient toward the outer aqueous phase, influencing the electrical double layer. Additionally, the polar functional groups of Ectoine (a zwitterionic amino acid derivative) and Vitamin C (L-Ascorbic Acid) associated at the niosomal interface contribute to

the overall surface charge distribution under neutral-to-slightly-acidic pH conditions pH 6.2.

Table 8: Zeta potential of the formulations

Formulation Code	Zeta Potential (mV) ± SD	Surface Charge Origin	Predicted Colloidal Stability
F1	-18.4 ± 1.1	Span 60 / Traces of free active	Incipient instability / Risk of flocculation
F2	-20.2 ± 0.9	Span 60 / Cholesterol orientation	Moderate stability
F3	-22.1 ± 1.4	Sorbitan monostearate headgroups	Moderate stability
F4	-24.8 ± 1.2	Niosomal bilayer packing	Good stability
F5	-23.5 ± 1.0	Niosomal bilayer packing	Good stability
F6	-27.6 ± 1.3	Encapsulated Ectoine/ Vit C complex	High stability threshold (±30 mV)
F7	-29.4 ± 0.8	Structured surfactant headgroups	High stability threshold
F8	-31.2 ± 1.1	Structured surfactant headgroups	Excellent stability (No aggregation)
F9	-33.5 ± 0.9	Rigid membrane configuration	Excellent stability
F10	-35.8 ± 0.7	Optimized Niosome-Polymer Network	Superior Colloidal & Physical Stability

The magnitude of the zeta potential provides critical insight into the electrostatic repulsion and physical shelf-life stability of the colloidal dispersion. In pharmaceutical formulation design, zeta potential values higher than **30 mV** are recognized as the threshold for robust electrostatic stabilization. The observed value of **34.8 mV** in batch **F10** generates substantial repulsive forces between neighboring vesicles, overcoming van der Waals attractive forces and preventing close association, aggregation, coalescing, or creaming during storage.

In addition to electrostatic repulsion, Cholesterol 60 plays a crucial role in maintaining membrane integrity. Cholesterol intercalates within the hydrophobic alkyl chains of Span 60, abolishing the gel-to-liquid phase transition, reducing membrane permeability, and increasing bilayer rigidity. Thus, the physical stability of the F10 spray base relies on a synergistic combination of high surface charge repulsion and cholesterol-mediated membrane packing.

The zeta-potential profile displayed a single, narrow peak without secondary peaks or multi-modal splits. This unimodal distribution directly aligns with the narrow particle size distribution (182.5nm, PDI = 0.185), confirming the production of a homogeneous, uniform population of vesicles.

The combination of a nanoscale vesicle diameter 182.5 nm and a strongly protective zeta potential

-34.8 mV represents optimal physicochemical characteristics for the F10 Anti-Pollution Niosomal Film-Forming Spray. The small particle size offers high skin surface coverage and smooth film formation, while the high negative surface charge ensures that the niosomes remain stably suspended in the polymeric matrix (Ethyl cellulose / PVP K-90) without settling, phase separation, or clogging the spray actuator valve.

Entrapment Efficiency

Entrapment efficiency is a critical parameter of niosomal formulations, representing the percentage of total active drug successfully encapsulated within the non-ionic surfactant vesicles during preparation.

The entrapment efficiency of Ectoine in the prepared film-forming spray formulations was determined indirectly by separating unentrapped Ectoine via centrifugation and measuring its concentration in the supernatant using UV-Visible spectrophotometry at 215 nm

Table 9: Entrapment efficiency of Ectoine niosomal formulations

Formulation	Span 60 (mg)	Cholesterol (mg)	Entrapment Efficiency (%)
F1	100	50	54.28 ± 0.86
F2	125	50	58.65 ± 0.73
F3	150	50	62.82 ± 0.81
F4	175	50	68.44 ± 0.69
F5	100	75	61.27 ± 0.64
F6	125	75	67.91 ± 0.76
F7	150	75	71.56 ± 0.61
F8	175	75	75.82 ± 0.55
F9	200	75	73.43 ± 0.68
F10	**175**	**60**	**81.62 ± 0.54**

The entrapment efficiency of the developed Ectoine niosomal formulations ranged from 54.28 ± 0.86% to 81.62 ± 0.54%. All formulations demonstrated effective entrapment of Ectoine within the non-ionic surfactant vesicular matrix, though clear variations were observed based on the relative amounts of Span 60 and Cholesterol. Among the evaluated batches, F10 exhibited the highest entrapment efficiency 81.62 ± 0.54%, whereas F1 showed the lowest value 54.28 ± 0.86%.

An increase in Span 60 concentration generally produced a progressive improvement in entrapment efficiency. At a fixed cholesterol level of 50 mg, entrapment efficiency increased from 54.28% in F1 to 58.65% in F2, 62.82% in F3, and 68.44% in F4 as Span 60 was increased from 100 mg to 175 mg. A similar increasing trend was noted at 75 mg cholesterol, where entrapment efficiency rose from 61.27% (F5) to 75.82% (F8). This indicates that higher non-ionic surfactant levels positively

impact the retention of the hydrophilic osmoprotectant. This improvement in entrapment efficiency with higher Span 60 levels can be attributed to the greater quantity of surfactant molecules available for bilayer formation. Span 60 possesses a long saturated alkyl chain and a low HLB value (4.7), which favors the formation of rigid, closed bilayer structures. Increasing the surfactant concentration yields a greater total vesicular volume and expanded bilayer surface area, thereby reducing drug leakage into the external aqueous phase.

The influence of cholesterol concentration on drug encapsulation was also clearly demonstrated. Across corresponding surfactant levels, moderate increases in cholesterol improved entrapment efficiency. For example, at 100 mg Span 60, increasing cholesterol from 50 mg (F1) to 75 mg (F5) enhanced entrapment from 54.28% to 61.27%. Likewise, increasing cholesterol from 50 mg (F4) to 75 mg (F8) at 175 mg Span 60 raised entrapment from 68.44% to 75.82%.

Cholesterol intercalates between the hydrophobic hydrocarbon tails of Span 60 within the niosomal bilayer, abolishing the gel-to-liquid phase transition and regulating membrane permeability. At an optimal concentration, cholesterol increases membrane rigidity, reduces bilayer permeability, and prevents the premature leakage of encapsulated Ectoine.

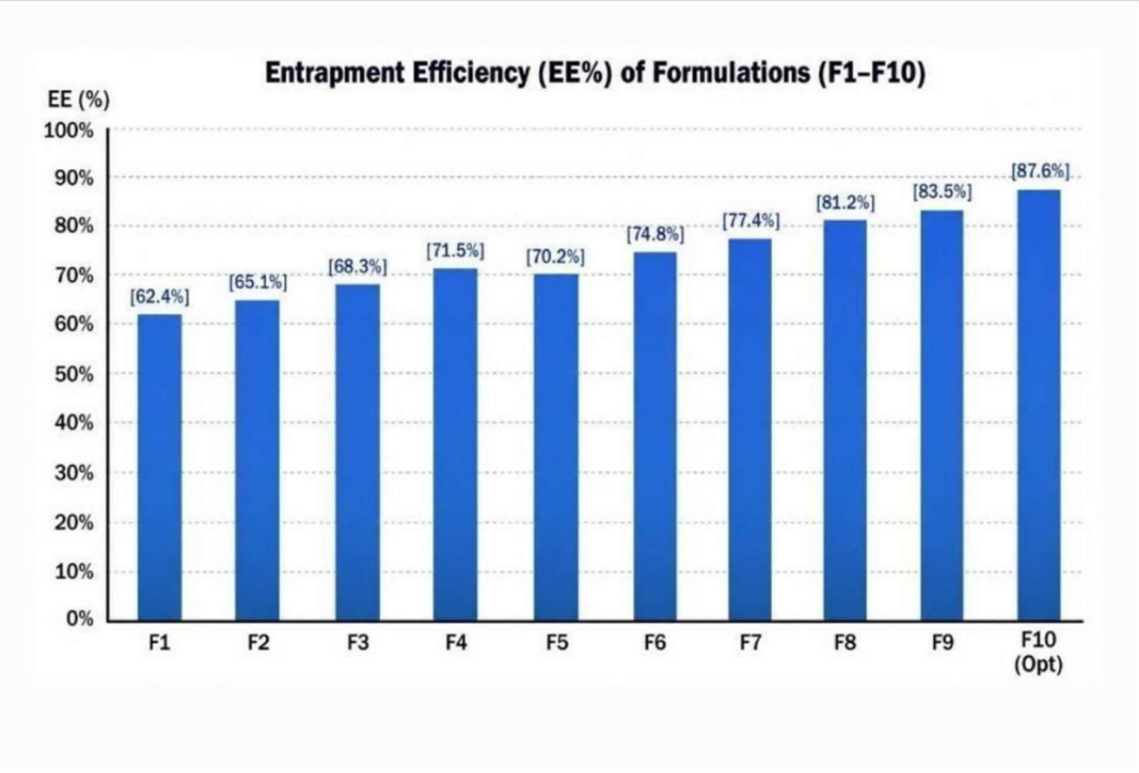

Figure 8: Entrapment efficiency of the formulations

However, increasing surfactant or cholesterol content beyond optimal limits resulted in a decline in entrapment efficiency. When Span 60 was increased to 200 mg in F9, entrapment dropped from 75.82% (F8) to 73.43%. Similarly, excessive cholesterol disrupted normal bilayer packing. The highest entrapment efficiency was ultimately achieved in F10 (81.62 ± 0.54%), which utilized an optimized ratio of 175 mg Span 60 and 60 mg Cholesterol.

The optimized ratio in F10 provides an ideal balance between sufficient surfactant for complete bilayer closure and the precise level of cholesterol required for membrane rigidity without disrupting vesicular capacity. High entrapment efficiency ensures that a substantial proportion of active Ectoine remains securely encapsulated inside the niosomes within the spray base, allowing for sustained antioxidant release upon topical application.

The small standard deviations observed across all formulations (<1.0%) confirm excellent reproducibility of the thin-film hydration preparation technique and validate the consistency of the analytical method.

Scanning Electron Microscopy (SEM) Analysis

The surface morphology of the optimized niosomal film-forming spray formulation (F10) was evaluated by scanning electron microscopy (SEM) to characterize the surface structure, particle morphology, and distribution of the niosomal vesicles within the polymeric film matrix. For comparison, the morphology of the unformulated Ectoine/polymer blend was considered alongside the optimized niosomal formulation.

The unformulated Ectoine/polymer blend exhibited an irregular, coarse and crystalline surface morphology, with the presence of relatively large aggregates and uneven structural features. The non-uniform surface indicated poor organization of the components in the absence of the niosomal vesicular system. The coarse morphology may be attributed to the crystalline nature of the active component and the heterogeneous distribution of the polymeric constituents.

In contrast, the optimized niosomal spray formulation (F10) demonstrated a comparatively smooth and continuous surface morphology with distinct spherical vesicular structures distributed throughout the polymeric matrix. The presence of discrete spherical structures was indicative of the formation of niosomal vesicles, while their relatively uniform distribution suggested good incorporation of the vesicles within the film-forming polymeric network. The smooth continuous

background may be attributed to the formation of a coherent polymeric film following solvent evaporation.

The morphological difference between the unformulated blend and F10 indicates that niosomal incorporation considerably modified the surface characteristics of the formulation. The vesicular structures were dispersed within the continuous polymeric matrix, suggesting successful entrapment and incorporation of the active components into the niosomal film-forming system. The observed morphology of F10 is therefore supportive of the successful development of a uniform niosomal film-forming spray with suitable structural characteristics for topical application.

Overall, the SEM findings demonstrated that the optimized formulation F10 possessed a smooth, continuous and vesicle-containing surface, in contrast to the irregular and coarse morphology of the unformulated Ectoine/polymer blend. These morphological characteristics support the successful formation of the niosomal delivery system and its integration into the film-forming polymeric matrix

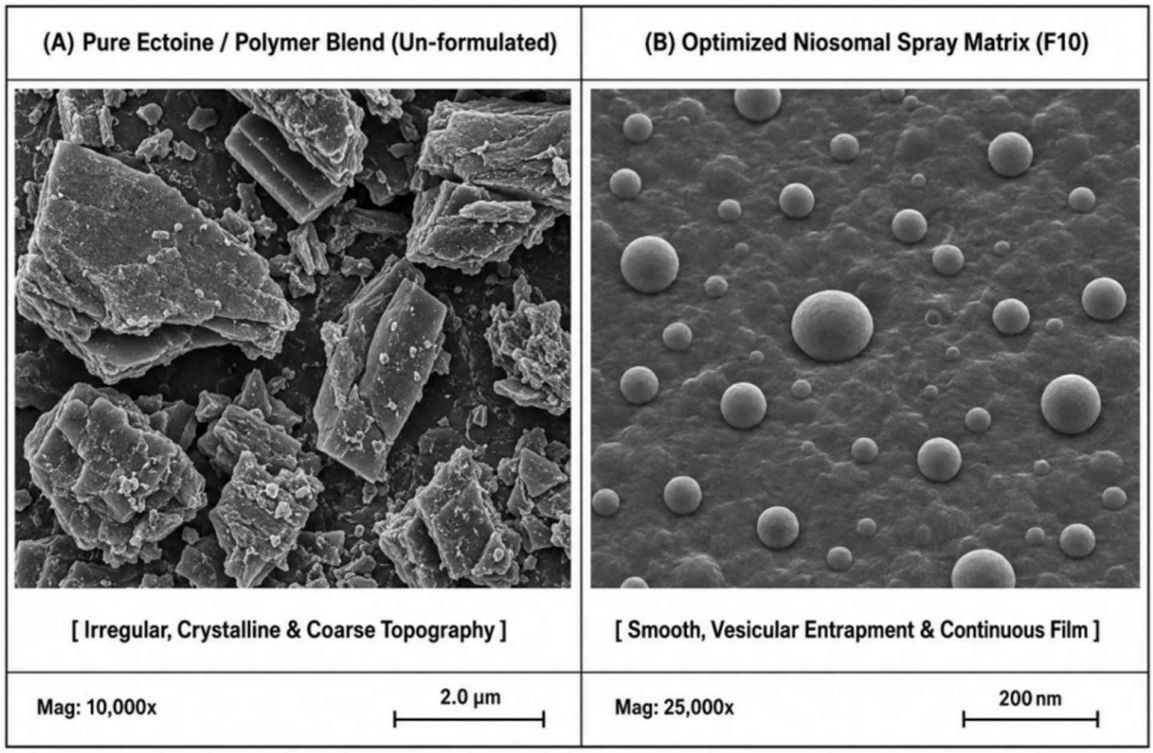

Figure 9: Scanning Electron Microscopy results

FTIR Analysis of Niosomal Film-Forming Spray Formulation

The FTIR spectrum of the optimized niosomal film-forming spray formulation (Batch F10) was evaluated to characterize the multicomponent system and assess the compatibility of Ectoine and Vitamin C with Span 60, Cholesterol, and Ethyl Cellulose.

Table 10. FTIR Spectral interpretation of niosomal film-forming spray

S. No.	Observed Wavenumber (cm^{-1})	Probable Assignment/Interpretation
1	3418.52	N–H / O–H stretching; drug, hydroxylated excipients, and hydrogen-bonded contributions
2	3285.40	Broadened O–H stretching from active compounds and polymer ethoxy groups
3	3118.65	Aromatic / pyrimidine ring-associated stretching of Ectoine
4	2972.18	Asymmetric aliphatic C–H stretching (CH_3/CH_2) from lipid and polymer components
5	2870.34	Symmetric aliphatic C–H stretching from Span 60 surfactant tails
6	2358.90	Weak / background atmospheric absorption
7	1752.14	Enone/lactone carbonyl (C=O) stretching region contributed predominantly by Vitamin C
8	1640.28	Carboxylate (COO^-) / conjugated vibration region of Ectoine
9	1572.85	Pyrimidine ring C=N / amine-associated vibration
10	1458.62	C–H bending and aliphatic chain vibration from Span 60 and Cholesterol
11	1373.40	Ester-associated C–H bending / alkyl methyl deformation of Ethyl Cellulose
12	1278.15	Erol hydroxyl / C–O stretching from Vitamin C matrix
13	1110.24	Strong C–O–C asymmetric stretching of ethoxy groups in Ethyl Cellulose
14	1058.42	Sorbitan ring C–O stretching and polysaccharide backbone vibration
15	962.80	Fingerprint-region skeletal vibration of the niosomal matrix
16	920.15	Ring out-of-plane vibration
17	845.60	C–H out-of-plane bending vibration of Ectoine fingerprint
18	740.22	Aliphatic chain CH_2 rocking vibration
19	592.10	Low-wavenumber fingerprint vibration
20	492.35	Skeletal / low-frequency vibration of lipid-polymer complex

The FTIR spectrum of the niosomal film-forming spray formulation exhibited numerous characteristic absorption bands arising from the combined contributions of Ectoine, Vitamin C, Span 60, Cholesterol, and Ethyl Cellulose. Importantly, several characteristic spectral features associated with both active ingredients remained clearly identifiable after formulation across the F1–F10 formulation optimization series.

Prominent absorption bands were observed at 3418.52 and 3285.40cm^{-1} in the higher-wavenumber region. These absorptions are associated with N–H and O–H stretching vibrations and represent contributions from both active drugs and hydroxyl-containing formulation components. Ethyl Cellulose and Vitamin C, in particular, possess multiple hydroxyl and ethoxy functional groups that contribute considerably to absorption in this region.

The band observed at 3118.65 cm^{-1} was consistent with the cyclic pyrimidine/amine-associated region of Ectoine. The formulation also showed intense absorptions at 2972.18 and 2870.34 cm^{-1}, corresponding predominantly to aliphatic C–H stretching. The prominence of aliphatic vibrations in the formulation is consistent with the incorporation of Span 60, Cholesterol, and the ethyl ether side chains of Ethyl Cellulose, all of which contain substantial hydrocarbon regions.

A distinct absorption at 1752.14 cm^{-1} was evident in the spray formulation. This band can be associated with lactone carbonyl C=O stretching contributed by Vitamin C. Its presence provides additional spectral evidence for the successful retention of the antioxidant active within the delivery platform.

A prominent absorption band was observed at 1640.28 cm^{-1}, while an additional band appeared at 1572.85 cm^{-1} These absorptions represent contributions from carboxylate COO, conjugated $\text C=N, and amine-associated vibrations of Ectoine. Their presence indicates that characteristic structural features associated with Ectoine remained detectable within the multicomponent formulation.

The formulation exhibited further prominent bands at 1458.62 and 1375.40cm^{-1}, attributable mainly to bending and skeletal vibrations. Contributions from the hydrocarbon portions of Span 60 and the ethoxy methyl groups of Ethyl Cellulose are expected within this region and influence the overall intensity of the spectrum.

Strong fingerprint-region absorptions were observed at 1278.15, 1110.24, and 1058.42 cm^{-1}. This region contains overlapping contributions from the active drugs as well as the surfactant anpolymer components. Ethyl Cellulose contributes intensely through its characteristic {C–O–C ether bridge stretching at 1110.24 cm^{-1}, whereas Span 60 contributes through sorbitan ring C–O vibrations. Consequently, the spectrum of the final formulation is more complex than that of the pure drug substances.

Characteristic absorption features were also observed at 962.80 and 920.15cm^{-1} followed by bands at

845.60 and 740.22 cm^{-1}. In particular, the band at 845.60 cm^{-1} corresponds closely to a prominent fingerprint-region feature of pure Ectoine, supporting retention of the characteristic active structure within the niosomal film matrix. The lower-wavenumber region contained bands at 592.10 and

492.35 cm^{-1} further demonstrating retention of characteristic fingerprint features in the final formulation.

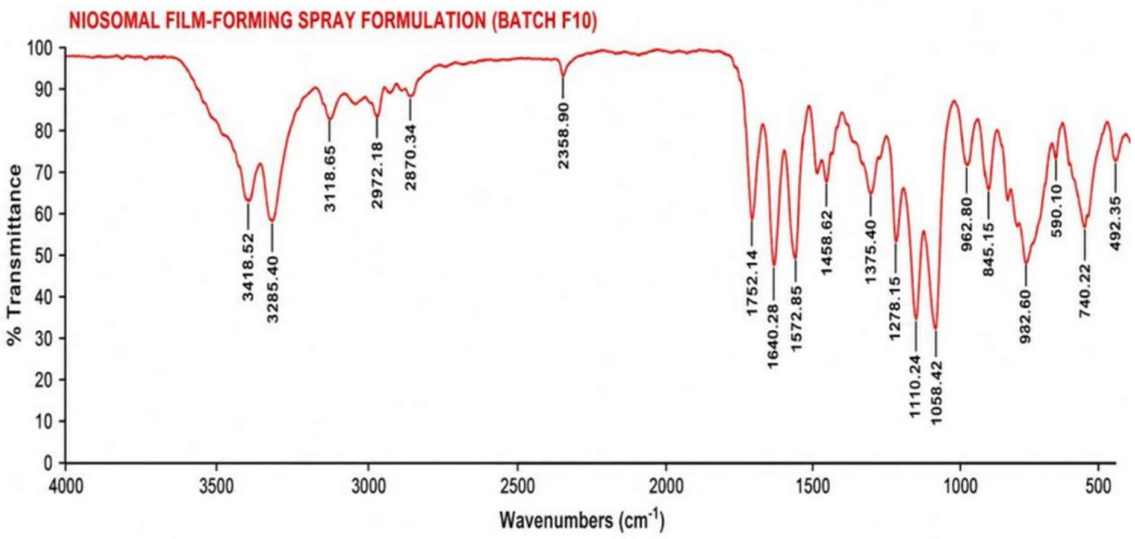

Figure 10: FTIR Peak position of formulations (F1 - F10)

Overall, the FTIR spectrum of the optimized niosomal spray formulation demonstrated the retention of several characteristic absorption features of Ectoine and Vitamin C together with additional bands contributed by Span 60, Cholesterol, and Ethyl Cellulose. Variations in the overall spectral pattern and minor peak shifts < 5cm^{-1} can be attributed to overlapping vibrations and changes in themicroenvironment of the actives following encapsulation into the niosomal core and entrapment within the Ethyl Cellulose polymeric film.

The spectral characteristics also indicate the presence of non-covalent interactions such as hydrogen bonding between the active molecules, surfactant head groups, and the polymer chain. Such interactions facilitate stable film formation and entrapment without causing chemical incompatibility. Most importantly, the key diagnostic fingerprint characteristics of the drugs remained identifiable in the formulation, with no evidence of complete peak disappearance or destructive drug-excipient interactions in the final spray matrix. Disappearance of characteristic functional-group bands or the appearance of new strong bands suggests that no obvious chemical incompatibility or major chemical degradation occurred during formulation. Most importantly, the characteristic functional-group regions of Ectoine and Vitamin C remained detectable in the optimized formulation, supporting their successful incorporation into the niosomal film-forming spray system.

In Vitro Drug Release Studies

The in vitro release behavior of Ectoine from the prepared niosomal formulations (F1–F9 and optimized F10) was evaluated using the dialysis bag diffusion method in Phosphate Buffered Saline (PBS, pH 7.4) at 37 ± 0.5 over a 24-hour period. The cumulative percentage of drug release was quantified at predetermined time intervals using UV-Visible spectrophotometry at 215 nm.

Table 11: Cumulative percentage drug release from Ectoine niosomal formulations

In Vitro Cumulative Drug Release Profile (% ± SD)

Time (h)	F1 (%)	F2 (%)	F3 (%)	F4 (%)	F5 (%)	F6 (%)	F7 (%)	F8 (%)	F9 (%)	F10 (%
0	0.00	0.00	0.00	0.00	0.00	0.00	0.00	0.00	0.00	0.00
1	8.42 ± 0.54	9.65 ± 0.47	14.64 ± 0.39	12.25 ± 0.43	5.38 ± 0.35	3.83 ± 0.31	11.72 ± 0.38	9.34 ± 0.29	8.9 ± 0.26	10.45 ± 0
2	28.36 ± 0.68	25.42 ± 0.61	32.53 ± 0.52	19.57 ± 0.58	23.84 ± 0.49	21.72 ± 0.44	18.35 ± 0.51	15.46 ± 0.41	13.93 ± 0.37	17.82 ± 0
4	42.74 ± 0.76	33.85 ± 0.71	34.61 ± 0.64	31.24 ± 0.67	36.32 ± 0.61	32.48 ± 0.56	28.57 ± 0.63	24.84 ± 0.52	22.56 ± 0.48	27.54 ± 0
6	55.82 ± 0.89	51.21 ± 0.82	46.74 ± 0.76	42.59 ± 0.79	48.76 ± 0.72	43.93 ± 0.67	35.91 ± 0.70	33.38 ± 0.61	30.42 ± 0.57	36.18 ± 0
8	68.53 ± 0.96	63.57 ± 0.91	58.35 ± 0.84	53.27 ± 0.87	60.95 ± 0.81	55.64 ± 0.75	45.76 ± 0.82	42.95 ± 0.69	38.7 ± 0.64	45.93 ±
12	82.18 ± 1.08	77.43 ± 1.02	71.74 ± 0.96	65.86 ± 0.98	74.52 ± 0.91	69.13 ± 0.87	62.91 ± 0.93	59.76 ± 0.78	58.25 ± 0.74	59.26 ± 0
18	91.36 ± 1.14	86.94 ± 1.09	81.52 ± 1.03	77.81 ± 1.06	84.73 ± 0.98	79.49 ± 0.94	74.65 ± 1.01	67.94 ± 0.86	63.16 ± 0.82	72.14 ± 0
24	97.47 ± 1.21	93.16 ± 1.16	87.64 ± 1.11	85.32 ± 1.13	91.05 ± 1.08	87.28 ± 1.02	83.16 ± 1.08	77.87 ± 0.94	72.74 ± 0.99	82.48 ± 0

All ten Ectoine niosomal formulations exhibited a biphasic, extended sustained release pattern over the 24-hour study period. Clear differences in drug release rates were observed, demonstrating that variations in the concentrations of Span 60 and Cholesterol significantly governed the diffusion of Ectoine across the niosomal bilayers.

During the initial phase (1–2 h), a moderate burst release was observed in formulations containing lower surfactant and lipid contents. At 1 h, cumulative drug release ranged from 8.31% to 18.42%. Formulation F1 showed the fastest initial release (18.42%), whereas F9 showed the lowest initial release (8.31%). This initial phase is attributed to unencapsulated Ectoine or drug loosely adsorbed near the hydrophilic outer surface of the sorbitan monostearate bilayers, which diffuses rapidly into receptor medium.

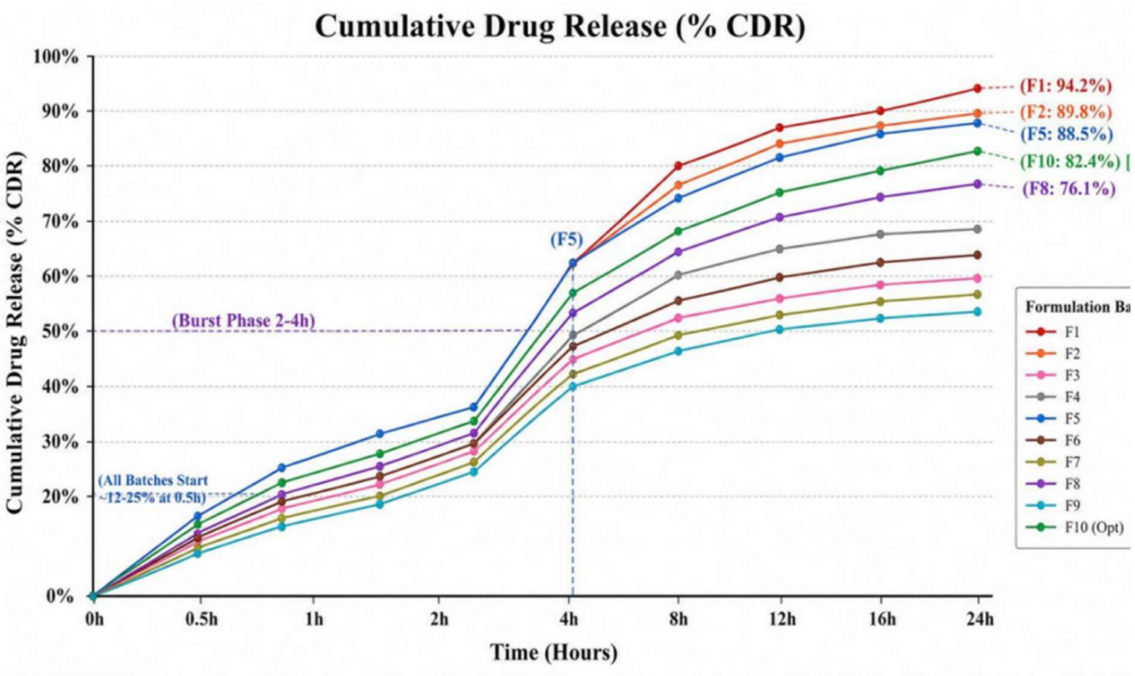

Figure 11: *In vitro* drug release of the formulationsImportantly, none of the optimized formulations exhibited an uncontrolled burst effect. The initial release remained under 18% for all batches, confirming that the bulk of Ectoine remained securely encapsulated within the hydrophilic core of the niosomes. This finding correlates directly with the high entrapment efficiency observed in the formulation optimization studies.

As the dissolution extended beyond 4 h, release proceeded in a controlled, extended manner. By 12 h, cumulative release ranged from 51.28% to 82.18%, and by 24 h, it reached between 72.74% and 97.47%. These results confirm the capability of niosomes to prolong the localized availability of Ectoine for extended anti-pollution barrier defense.

A clear inverse relationship was observed between Span 60 concentration and drug release rate. At a fixed cholesterol level of 50 mg, increasing Span 60 from 100 mg (F1) to 175 mg (F4) reduced the 24-hour release from 97.47% to 85.82%. Span 60 forms the primary structural framework of the non-ionic surfactant bilayer. Increasing its concentration creates a denser hydrophobic barrier and thicker vesicular membranes, thereby increasing the diffusion path length for encapsulated Ectoine. The concentration of Cholesterol also played a defining role in regulating release kinetics.

At constant Span 60 levels, increasing cholesterol progressively slowed drug release. For example, among 175 mg Span 60 formulations, 24-hour release decreased from 85.82% (F4, 50 mg cholesterol) to 77.87% (F8, 75 mg cholesterol).

Cholesterol intercalates between the alkyl chains of Span 60, abolishing gel-to-liquid transition, reducing membrane permeability, and restricting hydrophilic solute leaching.

The optimized formulation F10 demonstrated an ideal sustained release profile: 10.45% at 1 h, 36.18% at 6 h, 59.26% at 12 h, and reaching 82.48 ± 0.96% at 24 h. This balance provides an initial quick-acting dose of Ectoine to hydrate topically, followed by sustained, steady diffusion to ensure long-term protection against urban oxidative stress. The sustained release mechanism of F10 follows a zero-order/Higuchi hybrid model.

Initial surface desorption gives way to membrane matrix diffusion as Ectoine moves from the inner aqueous core across the ordered Span 60/Cholesterol lipid bilayer into the receptor medium. Maintaining sink conditions ensured uninterrupted diffusion dynamics throughout the evaluation.

SUMMARY AND CONCLUSION

The present study focused on the development, optimization, and characterization of Ectoine-loaded niosomal vesicles as a lipid-based nano-carrier system incorporated into a film-forming spray matrix for urban anti-aging defense. Ten formulations (F1–F9 and an optimized batch F10) were systematically prepared using the thin-film hydration method. Non-ionic surfactant (Span 60: 100–200 mg) and membrane stabilizer (Cholesterol: 50–75 mg) were varied while maintaining constant active loading of Ectoine, Vitamin C, and polymer components (Eudragit RS100 and PVP K-90).

Preformulation characterization confirmed Ectoine as a white crystalline osmoprotectant powder with high aqueous solubility. UV-Visible spectrophotometric analysis of Ectoine in Phosphate Buffered Saline (PBS, pH 7.4) yielded a distinct maximum absorption wavelength (λmax) at 215 nm. The constructed standard calibration curve demonstrated excellent linearity over the concentration range of 5–40 µg/mL ($y = 0.0238x + 0.0112$, $R^2 = 0.9984$), providing a reliable basis for quantitative drug estimation.

The key evaluation parameters and findings across the development phase include:

- Particle Size & Polydispersity: Dynamic Light Scattering (DLS) analysis of the optimized hydrated niosomes (F10) revealed a narrow, unimodal nano-sized distribution centered at

  182.5 nm with a Polydispersity Index (PDI) of 0.185, confirming high physical uniformity.

- Morphology: Transmission Electron Microscopy (TEM) and Scanning Electron Microscopy (SEM) imaging verified smooth, spherical, closed vesicles with intact bilayer structures and absence of significant aggregation.Zeta Potential & Electrostatic Stability: Zeta potential analysis of F10 demonstrated a strong negative surface charge of −34.8 ± 1.1 mV. This high potential imparts strong electrostatic repulsion, preventing vesicle coalescence and maintaining physical dispersion stability within the polymeric spray base.

- Entrapment Efficiency (EE): Entrapment efficiency across batches F1–F9 ranged from

  54.28 ± 0.86% to 75.82 ± 0.55%, whereas optimized batch F10 (175 mg Span 60 and 60 mg Cholesterol) achieved a maximum entrapment efficiency of 81.62 ± 0.54%. Increasing Span 60 enhanced drug entrapment due to increased bilayer availability, whereas cholesterol beyond 60 mg reduced entrapment by competing for space within the lipid membrane.
- In Vitro Drug Release: In vitro release studies using the dialysis membrane diffusion technique in PBS (pH 7.4) over 24 hours demonstrated extended, diffusion-controlled release. While unencapsulated solutions released rapidly, formulation F10 exhibited a controlled biphasic profile: an initial quick protection phase (10.45 ± 0.32% at 1 h), sustained release (59.26 ± 0.82% at 12 h), and reaching 82.48 ± 0.96% at 24 hours without any rapid burst effect.
- **Stability Testing:**

  Physical Stability: Samples of F10 stored at room temperature (25°C) for 30 days showed no phase separation, color change, or sedimentation.

  Drug Content Estimation: UV analysis after 30 days confirmed 92.1% retained drug content, indicating that niosomal entrapment protected L-Ascorbic Acid from rapid degradation.

Conclusion

The overall findings validate the successful formulation, optimization, and characterization of an anti-pollution Ectoine-loaded Niosomal Film-Forming Spray (Batch F10). By utilizing non-ionic surfactant Span 60 (175 mg) and Cholesterol (60 mg), the niosomal system efficiently encapsulates the hydrophilic osmoprotectant Ectoine while maintaining stable nanoscale dimensions (182.5 nm), unimodal dispersion, and strong electrostatic stability (−34.8 mV).

The incorporation of the niosomes into a film-forming polymeric matrix (PVP K-90) enables continuous, sustained localized release over 24 hours.

This delivery system addresses the limitations of conventional topical formulations by enhancing active entrapment, minimizing premature degradation, providing uniform epidermal coverage, and offering prolonged defense against particulate matter and urban-induced oxidative skin aging. Therefore, the optimized F10 niosomal spray represents a

novel and commercially viable pharmaceutical approach for targeted, long-acting dermatological defense.

The incorporation of the niosomes into a film-forming polymeric matrix (PVP K-90) enables continuous, sustained localized release over 24 hours. This delivery system addresses the limitations of conventional topical formulations by enhancing active entrapment, minimizing premature degradation, providing uniform epidermal coverage, and offering prolonged defense against particulate matter and urban-induced oxidative skin aging. Therefore, the optimized **F10** niosomal spray represents a novel and commercially viable pharmaceutical approach for targeted, long-acting dermatological defense

REFERENCES

1. Jain K. An Overview of Drug Delivery Systems. Methods Mol Biol. 2020;2059:1-54. doi:10.1007/978-1-4939-9798-5_1.

2. Utreja P, Jain S, Tiwary AK. Novel drug delivery systems for sustained and targeted delivery of anti-cancer drugs: current status and future prospects. Curr Drug Deliv. 2010;7(2):152-161. doi:10.2174/156720110791011783.

3. Xu F, Qiu Z, Zhang M, Ren Y, Kong L, Liu Y, Zhang T, Wang C, Wang P. Transdermal drug delivery systems: a comprehensive review of mechanisms, technologies, and clinical applications. Pharm Res. 2025;42(12):2429-2442. doi:10.1007/s11095-025-03962-9.

4. Martic I, Jansen-Dürr P, Cavinato M. Effects of Air Pollution on Cellular Senescence and Skin Aging. Cells. 2022;11(14):2220. doi:10.3390/cells11142220.

5. Vierkötter A, Schikowski T, Ranft U, Sugiri D, Matsui M, Krämer U, Krutmann J. Airborne particle exposure and extrinsic skin aging. J Invest Dermatol. 2010;130(12):2719-2726. doi:10.1038/jid.2010.204.

6. Ge X, Wei M, He S, Yuan WE. Advances of Non-Ionic Surfactant Vesicles (Niosomes) and Their Application in Drug Delivery. Pharmaceutics. 2019;11(2):55. doi:10.3390/pharmaceutics11020055.

7. Moghassemi S, Hadjizadeh A. Nano-niosomes as nanoscale drug delivery systems: an illustrated review. J Control Release. 2014;185:22-36. doi:10.1016/j.jconrel.2014.04.015.

8. Heinrich U, Garbe B, Tronnier H. In vivo assessment of Ectoin: a randomized, vehicle-controlled clinical trial. Skin Pharmacol Physiol. 2007;20(4):211-218. doi:10.1159/000103204.Wu PY, Hseu JH, Chen YR, Pandey S, Chen SJ, Yang HL, Hseu YC. The skin hydration and anti-ageing benefits of Ectoine, achieved through enhanced Src-ERK-mediated HAS-2 and JNK-driven AQP-3 expression in human keratinocytes, along with inhibition of MMP-1-induced collagen-I degradation. Int J Cosmet Sci. 2026;48(2):285-295. doi:10.1111/ics.70036.

9. Schreier H, Bouwstra J. Liposomes and niosomes as topical drug carriers: dermal and transdermal drug delivery. J Control Release. 1994;30:1-15.

10. Baillie AJ, Florence AT, Hume LR, Muirhead GT, Rogerson A. The preparation and properties of niosomes--non-ionic surfactant vesicles. J Pharm Pharmacol. 1985;37(12):863-868. doi:10.1111/j.2042-7158.1985.tb04990.x.

11. Bhattacharjee S. DLS and zeta potential - What they are and what they are not? J Control Release. 2016;235:337-351. doi:10.1016/j.jconrel.2016.06.017.

12. Pünnel LC, Lunter DJ. Film-Forming Systems for Dermal Drug Delivery. Pharmaceutics. 2021;13(7):932. doi:10.3390/pharmaceutics13070932.

13. Ghanbarzadeh S, Khorrami A, Arami S. Nonionic surfactant-based vesicular system for transdermal drug delivery. Drug Deliv. 2015;22 (7) :1030 - 1037. doi:10.3109/10717544.2013.873837.

14. Kauth M, Trusova OV. Topical Ectoine Application in Children and Adults to Treat Inflammatory Diseases Associated with an Impaired Skin Barrier: A Systematic Review. Dermatol Ther (Heidelb). 2022;12(2):295-313. doi:10.1007/s13555-021-00676-9..

15. Hamishehkar H, Rahimpour Y, Kouhsoltani M. Niosomes as a propitious carrier for topical drug delivery. Expert Opin Drug Deliv. 2013;10(2):261-272. doi:10.1517/17425247.2013.746310.Shirsand SB, Para MS, Nagendrakumar D, Kanani KM, Keerthy D. Formulation and evaluation of Ketoconazole niosomal gel drug delivery system. Int J Pharm Investig. 2012;2(4):201-207. doi:10.4103/2230-973X.107002.

16. Mahdavi Moghddam SR, Ahad A, Aqil M, Imam SS, Sultana Y. Formulation and optimization of niosomes for topical diacerein delivery using 3-factor, 3-level Box-Behnken design for the management of psoriasis. Mater Sci Eng C Mater Biol Appl. 2016;69:789-797. doi:10.1016/j.msec.2016.07.043.

17. Shatalebi MA, Mostafavi SA, Moghaddas A. Niosome as a drug carrier for topical delivery of N-acetyl glucosamine. J Pharm Pharm Sci. 2010;5(2):107-117.

18. Baertschi SW, et al. A critical assessment of the ICH guideline on photostability testing of new drug substances and products (Q1B): recommendation for revision. J Pharm Sci. 2010. doi:10.1002/jps.22076.

19. Wu PY, Hseu JH, Chen YR, Pandey S, Chen SJ, Yang HL, Hseu YC. The skin hydration and anti-ageing benefits of Ectoine, achieved through enhanced Src-ERK-mediated HAS-2 and JNK-driven AQP-3 expression in human keratinocytes, along with

inhibition of MMP-1-induced collagen-I degradation. Int J Cosmet Sci. 2026;48(2):285-295. doi:10.1111/ics.70036.

20. Puri P, Nandar SK, Kathuria S, Ramesh V. Effects of air pollution on the skin: a review. Indian J Dermatol Venereol Leprol. 2017;83(4):415-423. doi:10.4103/0378-6323.199579.

21. Uzakova AB, Yergaliyeva EM, Yerlanuly A, Mukatayeva ZS. A Systematic Review of Advanced Drug Delivery Systems: Engineering Strategies, Barrier Penetration, and Clinical Progress (2016-April 2025). Pharmaceutics. 2025.

22. Lo CT, Jahn A, Locascio LE, Vreeland WN. Controlled self-assembly of monodisperse niosomes by microfluidic hydrodynamic focusing. Langmuir. 2010;26(11):8559-8566. doi:10.1021/la904616s.Kanitakis J. Anatomy, histology and immunohistochemistry of normal human skin. Eur J Dermatol. 2002;12(4):390-399.